

Published in Physical Review C **51**, 1528 (1995)

## Positivity restrictions in polarized coincidence electronuclear scattering

V. Dmitrašinović

*Physics Department, University of Colorado,  
Nuclear Physics Lab, P.O. Box 446,  
Boulder, CO 80309-0446*

### Abstract

We make a systematic examination of the role played by the restriction that the cross section in polarized coincidence electronuclear processes must be positive. The necessary formalism for unpolarized scattering structure functions is developed within two frameworks: (i) the response tensor method, and (ii) the Jacob-Wick method. Equivalence of the two methods is demonstrated for unpolarized scattering, and then the simpler Jacob-Wick method is applied to the polarized pseudoscalar electroproduction off a nucleon. We derive three known and eight new inequalities among the polarized target structure functions, as well as eleven new polarized ejectile structure function inequalities. We also provide rules for this method to be used in the deuteron two-body electrodisintegration in conjunction with the results published in Phys. Rev. C **40** 2479 (1989).

PACS numbers: 25.30.-c, 24.70.+s, 13.60.-r

Typeset using REVTeX

## I. INTRODUCTION AND SUMMARY

The new and upgraded electron scattering facilities have revived interest in coincidence electronuclear scattering [1], and in polarization measurements in particular. In recent years we have seen a number of theoretical papers [2–4] on the general properties of such cross sections as expressed in three different formalisms. A fully relativistic method based on the Jacob-Wick helicity formalism [5] has been developed for several two-body final state reactions [2,6–10]. This method allows a comparatively straightforward separation of scattering amplitudes [2,8] from the polarization observables. Although, at this time complete experimental separation seems an excessively ambitious project for all but a few reactions with small spins, such theoretical analysis teaches us about the sensitivity of observables to certain amplitudes, and, as we will show in this paper, it allows the construction of model-independent inequalities among the observables. A technically different, but physically related, approach to polarized, coincidence, inelastic electron scattering was worked out by Donnelly and Raskin [3]. They use conservation of angular momentum in order to expand the transition amplitudes in terms of multipoles, and then write the cross section as a function of the latter. While this approach is closer to the traditional methods of nonrelativistic electronuclear physics [11], it is much more complicated than the helicity amplitude method and it does not allow a simple separation analysis. Furthermore, it is not unique insofar as such multipole analysis can also be completed starting from the Jacob-Wick helicity amplitudes [1,7]. Finally, a relativistic formalism for the description of target polarization in coincidence inelastic electron scattering based on the most general expansion of the response tensor was developed by De Rujula, Doncel and de Rafael [12]. This method, which follows the lines of de Forest’s [13] unpolarized coincidence analysis, has recently been extended to describe polarized recoil reactions by Picklesimer and van Orden [4], as well. The final state channels are not sufficiently well-specified for the separation of amplitudes to be feasible within this method. These three formalisms may look distinct, but they are essentially equivalent: they all rely on the one-photon-exchange approximation and the use of electromagnetic (EM) current conservation.

Despite of all this formal effort, precious few actual calculations [4,14,15] have been done, so that relatively little is known about the actual size, shape, and form of these polarized response functions in general. Furthermore, at least one aspect of the problem remains unexplored: constraints on the polarized structure functions due to the condition that the cross section be positive, or vanishing (“positive semi-definite”). The *inclusive unpolarized* structure functions are well known to be positive definite [11]. The polarized structure functions, although not positive definite, are also bounded by certain functions of the unpolarized ones [16], but these bounds are not widely known. As an example of potential usefulness, such “positivity” constraints were used in estimates of counting rates for measuring the polarized DIS structure function  $g_1$ , before the experiments. Some of the above mentioned coincidence scattering methods were developed along the lines of inclusive electron scattering, so we expect to find similar positivity constraints for coincidence structure functions.

In this paper we present one model-independent set of constraints in the form of inequalities among various structure functions based exclusively on the positive definiteness of scattering cross sections, *i.e.*, probabilities. Such inequalities have already been derived

for *unpolarized* and several of the *polarized target* coincidence structure functions [17]. One particularly interesting example (see Sect. II.B below) is the upper bound on the absolute value of the so-called “fifth structure function” given in terms of the remaining four unpolarized structure functions. These results are largely unknown in the nuclear physics community, so that they have not seen many applications so far. One of the purposes of this paper is to bring some awareness of these results to a wider audience. After all, these results are by no means obvious, as are their unpolarized inclusive counterparts, and are a natural consequence of the probabilistic nature of scattering cross section.

The method that was originally used [12,17] was based on the response tensor formalism and turned out to be increasingly complicated with the increase of the number of spin degrees of freedom. For that reason, no double-polarization experiment structure function inequalities are discussed here. We develop an alternative scheme based on the Jacob-Wick helicity formalism that is substantially simpler, especially in view of the fact that all of the polarization observables that are necessary for this purpose have already been worked out for two reactions [2,8]. In order to test the method, we first explicitly show its equivalence with the conventional (response tensor) method results for unpolarized coincidence scattering where *all* inequalities are already known. Then we extend our calculation to the polarized spin 1/2 ejectile case where we confirm five known inequalities and derive six new ones. These are by no means all of the inequalities one can derive in this way. We have only looked at the inequalities that involve up to trilinear products of structure functions whereas one can have products of up to six structure functions. Rather than spelling out all of them (they become increasingly complicated) we indicate how they can be extracted by the interested reader from the tables provided here, when the need arises. Then we repeat this exercise for polarized spin 1/2 target coincidence reactions. Finally, with regard to target spin 1 and ejectile spin 1/2 reaction the purpose of this paper is one of a do-it-yourself manual. We leave the majority of results to be constructed by the interested reader, as the need and occasion arise. For that purpose, Ref. [10] is meant to be used as the source of tables of polarization observables and their transformation properties.

This paper is organized as follows. In Section II we review the basics of the Jacob-Wick and response tensor based formalisms and then present two different derivations of the positivity conditions for the *unpolarized coincidence* structure functions in order to prove their equivalence. In Section III we explicitly construct the positivity conditions for spin 1/2 target and ejectile *polarized coincidence* structure functions using the second (simpler) of the two methods. We discuss our results and compare them with those of Ref. [12]. Then, we define rules for the derivation of spin 1 polarized target coincidence structure functions.

## II. REVIEW OF THE FORMALISM

In order to set the notational conventions, we review in subsection II.A. the basic results of the polarization observables analysis in  $(e, e'N)$  worked out within the Jacob and Wick helicity formalism in Refs. [9,2,10]. Then, in subsection II.B. we work out the general positivity constraints in unpolarized coincidence electron scattering.

### A. Polarization observables in coincidence electron scattering

The general form of the inelastic coincidence electron scattering cross section for arbitrary polarization of the target and/or ejectile, with two particles in the final state, in the “mixed” frame, *i.e.*, with electron variables in the laboratory (lab) and the hadronic variables in the centre-of-mass (c.m.) frame, is [2]

$$\begin{aligned} \frac{d^5\sigma}{d\Omega' dE' d\Omega_1} = & \frac{\sigma_M p_1}{4\pi M_T} \left\{ \left( \frac{W}{M_T} \right)^2 v_L R_L + v_T R_T + v_{TT} [\cos 2\phi R_{TT}^{(I)} + \sin 2\phi R_{TT}^{(II)}] \right. \\ & + \left( \frac{W}{M_T} \right) v_{LT} [\cos \phi R_{LT}^{(I)} + \sin \phi R_{LT}^{(II)}] \\ & \left. + 2h v'_T R_{T'} + 2h \left( \frac{W}{M_T} \right) v'_{LT} [\cos \phi R_{LT'}^{(II)} + \sin \phi R_{LT'}^{(I)}] \right\}, \end{aligned} \quad (1)$$

where  $p_1$  is the absolute value of the ejectile three-momentum in the c.m. frame and  $E_1$  is the corresponding ejectile energy,  $h = \pm 1/2$  is the helicity of the incoming electron,  $M_T$  is the target-nucleus mass,  $\sigma_M$  is the Mott cross-section

$$\sigma_M = \left( \frac{\alpha \cos \frac{1}{2}\theta}{2E \sin^2 \frac{1}{2}\theta} \right)^2,$$

and

$$\begin{aligned} v_L &= \left( \frac{Q^2}{q_L^2} \right)^2 & v_{TT} &= -\frac{1}{2} \left( \frac{Q^2}{q_L^2} \right) \\ v_{LT} &= -\frac{1}{\sqrt{2}} \left( \frac{Q^2}{q_L^2} \right) \sqrt{\frac{Q^2}{q_L^2} + \tan^2 \frac{1}{2}\theta} & v'_{LT} &= -\frac{1}{\sqrt{2}} \left( \frac{Q^2}{q_L^2} \right) \tan \frac{1}{2}\theta \\ v_T &= \frac{1}{2} \frac{Q^2}{q_L^2} + \tan^2 \frac{1}{2}\theta & v'_T &= \tan \frac{1}{2}\theta \sqrt{\frac{Q^2}{q_L^2} + \tan^2 \frac{1}{2}\theta}. \end{aligned} \quad (2)$$

The kinematic variables entering this cross-section are: the total c.m. energy of the system  $W = \sqrt{(P+q)^2}$  (here  $P_\mu$  is the target nucleus four-momentum), the negative four-momentum transfer squared  $Q^2 = -q^2 = \mathbf{q}_L^2 - \nu^2$ , the absolute value of the momentum transfer three-vector in the lab frame  $q_L = |\mathbf{q}_L|$ , the energy loss  $\nu = E - E'$ , the initial  $E$  and the final state electron energy  $E'$  in the lab frame, the electron scattering angle  $\theta$  in the lab frame, the ejectile opening angle  $\theta_1$  in the c.m. frame and the azimuthal angle  $\phi$  (see Fig. 1). We use Bjorken and Drell [18] metric and  $\alpha \simeq 1/137$  is the fine-structure constant. The only assumptions entering this result are (i) one-photon exchange approximation and (ii) conserved hadron electromagnetic (EM) current. Parity conservation has not been assumed as yet.

The response functions  $R$ 's are functions of  $W, Q^2$  and  $\theta_1$ , but not of  $\phi$ , as long as the target polarization is specified with respect to the coordinate system  $(x', y', z')$  (Fig. 1) and recoil polarization is measured with respect to the  $(x'', y'', z'')$  (Fig. 1) coordinate system. We emphasize this because the specification of the recoil polarization measurement coordinate

frame has recently been a source of some confusion<sup>1</sup>. Thus, the “interference”  $R$ ’s, which do have a  $\phi$ -dependent factor, can be separated by making measurements at different values of  $\phi$  and otherwise identical kinematics. The remaining “diagonal”  $R$ ’s that do not have a  $\phi$ -dependent factor can be separated by Rosenbluth separation. The structure functions  $R$  are linear combinations of functions  $R_{ab}$ , which in turn, are traces of products of helicity transition matrices  $\hat{J}_a, \hat{J}_b^\dagger$  (see Eq. (32) of Ref. [2]) and the density matrices of the initial and the final states:

$$R_{ab} = (2s_1 + 1)(2s_2 + 2) \kappa^2 \text{tr}\{\rho_f \hat{J}_a \rho_i \hat{J}_b^\dagger\}, \quad (3)$$

where  $\kappa^2 = M_1 M_2 / 4\pi^2 W$ ,  $M_{1,2}$ ,  $s_{1,2}$  are the masses and spins of the particles No. 1 (“ejectile”) and No. 2 (“residual nucleus”) in the final state, respectively, and all the density matrices are normalized to  $\text{tr}(\rho_{f,i}) = 1$ . Here the  $a, b$  indices stand for the helicities of the virtual photon. The density matrices can be expanded in terms of irreducible tensor operators (ITOs) (see Eqs. (37, 38, 45) of ref. [2]) as follows:

$$\rho_{i,f}(j) = \frac{1}{(2s_j + 1)} \sum_J \sum_M T_{JM}^*(j) \tau_{JM}(j) \quad (4)$$

where  $s_j$  is the spin value of the  $j^{\text{th}}$  particle in the initial, or the final state,  $\tau_{JM}(j)$  is the  $M^{\text{th}}$  component of the spherical ITO of rank  $J$ , and  $T_{JM}(j)$  are the corresponding components of the *polarization* spherical ITO. Lorentz boost transformation properties of the polarized observables have been worked out in Ref. [10]. Analogous transformation properties of unpolarized structure functions in coincidence electronuclear scattering were worked out by Walecka and Zucker [7] some time ago. Note that particles No. 2 in their respective two-body helicity states (the target particle in the initial state, and the “residual nucleus” in the final state) carry a tilde above the polarization ITO in order to indicate this fact.

All structure functions can be divided into two classes: class I structure functions ( $R_L$ ,  $R_T$  besides all other structure functions explicitly denoted as such by the superscript I) are nonzero in *unpolarized*, *parity conserving* reactions, while class II structure functions ( $R_{T'}$  besides all other structure functions explicitly marked II) vanish identically because of constraints imposed by parity. Once the polarization measurement is allowed, this rule is modified, but it remains true that one half of all possible structure functions vanish because of parity constraints.

## B. Unpolarized coincidence positivity inequalities

The differential cross section  $d\sigma$  is a positive or vanishing (positive semi-definite), quantity. Its general form in the one-photon-exchange approximation is proportional to  $l_\mu^* W^{\mu\nu} l_\nu$ ,

---

<sup>1</sup>It has been erroneously claimed in Ref. [19] that in the helicity formalism, the recoil polarization is to be measured with respect to the  $(x', y', z')$  coordinate system shown in Fig. 1. An independent calculation of the recoil polarization observables by O. Hanstein [20], using CGLN amplitudes, *i.e.* outside of the Jacob-Wick formalism, has shown a discrepancy with Lourie’s [19] results in exactly the form of a rotation through angle  $\theta_1$ . This simply and explicitly confirms our claim.

where  $l_\mu$  is the lepton current and  $W^{\mu\nu}$  is the Hermitian positive semi-definite response tensor. From these two facts alone one can derive nontrivial inequalities among the structure functions. For inclusive electron scattering the first comprehensive study of positivity constraints was published in Ref. [16]. In the following we will repeat the derivation of the unpolarized structure function inequalities using two different methods in order to establish their equivalence. The second method will prove to be much more practical for deriving new, *polarized* structure function inequalities. Some of the polarized target inequalities have already been given in Ref. [12], but all of the polarized ejectile and some of the polarized target inequalities presented here are new.

### 1. Positivity inequalities via response tensor method

Here we extend the original method of Doncel and de Rafael [16] to unpolarized *coincidence* scattering structure functions. The derivation of the positivity inequalities is accomplished by starting from the most *general* unpolarized coincidence cross section for *arbitrary* targets and final states that is expressed in terms of the so-called response tensor  $W^{\mu\nu}$ :

$$W^{\mu\nu} = -W_1 \tilde{g}^{\mu\nu} + W_2 \frac{\tilde{p}_T^\mu \tilde{p}_T^\nu}{p_T^2} + W_4 \frac{\tilde{p}_1^\mu \tilde{p}_1^\nu}{p_1^2} + W_3 \frac{1}{2p_T \cdot p_1} [\tilde{p}_T^\mu \tilde{p}_1^\nu + \tilde{p}_1^\mu \tilde{p}_T^\nu] + W_5 \frac{i}{2p_T \cdot p_1} [\tilde{p}_T^\mu \tilde{p}_1^\nu - \tilde{p}_1^\mu \tilde{p}_T^\nu], \quad (5)$$

where  $W_i$  ( $i = 1 - 5$ ) are the five real linearly independent response functions and

$$\tilde{g}^{\mu\nu} = g^{\mu\nu} - \frac{q^\mu q^\nu}{q^2}; \quad \tilde{p}^\mu = p^\mu - \frac{p \cdot q}{q^2} q^\mu.$$

The inelastic coincidence electron scattering cross section for arbitrary unpolarized target and arbitrary unpolarized ejectile, and any number of hadrons in the final state, in the lab frame that follows from the above response tensor is [13]

$$\frac{d^5\sigma}{d\Omega' dE' d\Omega_L} = \frac{\sigma_M p_L}{4\pi M_T} r \left\{ v_L R_L + v_T R_T + v_{TT} [\cos 2\phi R_{TT}^{(I)} + \sin 2\phi R_{TT}^{(II)}] + v_{LT} [\cos \phi R_{LT}^{(I)} + \sin \phi R_{LT}^{(II)}] + 2hv'_T R_{T'} + 2hv'_{LT} [\cos \phi R_{LT'}^{(II)} + \sin \phi R_{LT'}^{(I)}] \right\}, \quad (6)$$

where  $d\Omega_L, p_L$  are the differential solid angle subtended by, and the absolute value of the ejectile lab three-momentum, respectively, and the recoil factor  $r$  (see Eq. (94) of Ref. [2])

$$r = \frac{W}{M_T} \left( 1 + \frac{\nu p_1 - E_1 q \cos \theta_1}{M_T p_1} \right)_L^{-1}$$

only appears if the final state contains two hadrons. The structure functions  $R$ 's are evaluated in the lab frame, and are shown in Table II. This differs from the cross section in the “mixed” , *i.e.*, c.m. and lab frames through the absence of  $W/M_T$  factors in front of the longitudinal structure functions (see Eq. (94) of Ref. [2]) and a different  $\eta$  factor in Table I (see below).

We could directly proceed from  $l_\mu^* W^{\mu\nu} l_\nu \geq 0$  to find the positivity conditions. Note, however, that  $W_{\mu\nu}$  has only nine independent elements despite being a  $4 \times 4$  matrix. This, of course, is a consequence of gauge invariance, which relates the longitudinal and the scalar (zeroth) components of this tensor. Nevertheless, in general, all 16 matrix elements are nonzero. The key to simplification, as suggested by Doncel and de Rafael [16], is to explicitly reduce this four-dimensional matrix to a three-dimensional one by a clever choice of reference frame. One solution is to work in the Breit frame where the four-vector  $q_\mu$  loses its temporal component and becomes

$$q_B^\mu = (0, \mathbf{q}_B) = (0, 0, 0, Q) .$$

Then, the current conservation condition

$$q_\mu W^{\mu\nu} = q_\nu W^{\mu\nu} = 0$$

turns into

$$W_B^{3,\nu} = W_B^{\mu,3} = 0,$$

*i.e.*, only the first three rows and columns survive. It turns out that this solution can be made frame-independent by introducing the covariant photon helicity zero amplitudes. That fact will be proven and used later on,

By finding the relation between the  $R$ 's in the lab frame and the response tensor  $W_{\mu\nu}$  in the Breit frame, we express all of the elements of  $W_{\mu\nu}$  in terms of the observed lab frame  $R$ 's. So, the first step is to work out the boost to the Breit frame. We see that the lab→Breit boost is along the  $z$  axis so that only the zeroth component is influenced, just like the lab→c.m. boost worked out in Ref. [2] (see Eq.(20) therein). Once again the whole effect of the boost is reduced to multiplicative factors in front of the L and LT structure functions and a different phase space factor which is unimportant for this purpose. To find the multiplicative factor  $\eta$  appropriate to the Breit frame we go through the same procedure as in Sec. II.B. of Ref. [2]. The Breit frame is defined by

$$q_B^\mu = (0, 0, 0, q_B) ,$$

whereas in the lab frame,  $p_{1L}^\mu = (M_T, \mathbf{0})$ . The boost transformation is shown in matrix form as

$$B_B = \begin{pmatrix} \frac{q_L}{Q} & 0 & 0 & \frac{-\nu}{Q} \\ 0 & 1 & 0 & 0 \\ 0 & 0 & 1 & 0 \\ \frac{-\nu}{Q} & 0 & 0 & \frac{q_L}{Q} \end{pmatrix} ,$$

so that, if  $q_L^\mu = (\nu, 0, 0, q_L)$ , then

$$q_B = B_B q_L = \frac{q_L}{Q} q_L - \frac{\nu}{Q} \nu = Q ,$$

and we find  $\eta = 1$  in the Breit frame, whereas  $\eta = \frac{q_L}{Q}$  is appropriate to the lab frame (see Eq.(94) in [2]), and  $\eta = \left(\frac{q_L}{Q}\right) \left(\frac{M_T}{W}\right)$  in the c.m. frame (see Eq.(29) in [2]). The transverse helicity amplitudes are unchanged by these boosts, and  $\epsilon_o^B$  in the Breit frame is the time-like unit four-vector  $\epsilon_o^{\mu B} = (1, \mathbf{0})$ . This means that the zeroth component of the response tensor in the Breit frame is equivalent to the Lorentz-invariant scalar product (contraction) of the

covariant zero-helicity polarization four-vector and the covariant response tensor. This fact will be used later on to define Lorentz-invariant inequalities.

The second simplification used is the rotation of the response tensor about the  $z$ -axis through  $\phi$  which is described in detail in Ref. [2], so it will not be dwelt on here. The rotation does not change the positivity conditions because it is an orthogonal coordinate transformation. The response tensor defined with respect to the azimuthally rotated coordinate system  $(x', y', z')$  of Fig. 1 will be denoted by  $w_{\mu\nu}$ . The relationship between the observables and the response tensor matrix elements in the Breit frame is given in Table III. This result allows us to invert these relations and express the response tensor matrix elements, *i.e.*, response functions in terms of observables.

Now that we have reduced the response tensor to a three-dimensional matrix with elements expressed in terms of observables, we can apply the mathematical machinery of positivity constraints on quadratic forms. The mathematical statement that a quadratic form (matrix) is positive semi-definite is equivalent to the statement that all of its principal minors are positive semi-definite, *i.e.*, positive or zero. This is easily proven by diagonalizing the quadratic form and remembering that determinants (minors) do not change under similarity transformations, *i.e.*, under rotations of the basis of the linear space.

A direct evaluation of the principal minors of the response tensor yields the following inequalities (all  $w$ 's are in the Breit frame and their relation to the observables is given in Table III):

$$w_{00}, w_{xx}, w_{yy} \geq 0 \quad (7a)$$

$$\begin{vmatrix} w_{00} & w_{0x} \\ w_{x0} & w_{xx} \end{vmatrix} \geq 0 \quad (7b)$$

$$\begin{vmatrix} w_{00} & 0 \\ 0 & w_{yy} \end{vmatrix} \geq 0 \quad (7c)$$

$$\begin{vmatrix} w_{xx} & 0 \\ 0 & w_{yy} \end{vmatrix} \geq 0 \quad (7d)$$

$$\begin{vmatrix} w_{00} & w_{0x} & 0 \\ w_{x0} & w_{xx} & 0 \\ 0 & 0 & w_{yy} \end{vmatrix} \geq 0, \quad (7e)$$

Note that only inequalities (7a,b) are independent; the remaining two inequalities (7c,d) being derivable from the first four. This, together with the hermiticity of the response tensor ( $w_{\mu\nu} = w_{\nu\mu}^*$ ), leads to inequalities Eq. (8a-c, 10). Specifically, from Eq. (7a) and Table III we conclude that

$$R_L \geq 0 \quad (8a)$$

$$R_T \geq 0 \quad (8b)$$

$$R_T \geq |R_{TT}^{(I)}|. \quad (8c)$$

On the other hand, from Eq. (7b) and Table III we obtain:

$$w_{00}w_{xx} \geq |w_{0x}|^2 \quad (9)$$

$$4R_L [R_T - R_{TT}^{(I)}] \geq (R_{LT}^{(I)})^2 + (R_{LT'}^{(I)})^2 \quad (10)$$



which completes our derivation. All of these results hold at each and every kinematic point, *i.e.*, for every  $W^2, \theta_1, Q^2$ .

We will re-derive these very same inequalities using a seemingly different method and thus establish the equivalence of the methods. This second method turns out to be much more economical for deriving new, *polarized* structure function inequalities. Some of the “polarized target” inequalities have already been written down in Ref. [17], but all of the polarized ejectile and some of the polarized target inequalities presented here are new.

## 2. Positivity inequalities via helicity density matrix method

In the previous section we have intentionally used the helicity states and helicity formalism wherever possible so as to simplify the calculation. Specifically, we have discovered that the linearly independent components of the response tensor can be rearranged into covariant helicity eigenstates without spoiling the positivity properties. We build our second method on that simple observation. It is important to realize that the transition from the Cartesian response tensor to the photon helicity states is just an orthogonal coordinate transformation that does not change the positivity relations. Furthermore, by using covariant helicity states of the photon, the whole method becomes frame-independent. Rewriting Eqs.(7a-d) into the helicity (“spherical tensor”) basis we realize that this is just the positivity constraint for the virtual photon density matrix. Density matrices are observables, so they must be Hermitian. Moreover, they must be positive semi-definite: the elements of the diagonalized density matrix are *probabilities* of the system being in the given pure state, and probabilities have to be positive, or zero.

Working in the virtual photon helicity basis, we find the relationship between the structure functions  $R$ ’s in the lab frame and the rotated response tensor matrix elements in the Breit frame that is shown in Table IV. In the helicity basis, the response tensor in the ejectile plane is

$$\rho_{\lambda'\lambda} = \varepsilon_\mu^*(\lambda') w^{\mu\nu} \varepsilon_\nu(\lambda) = \begin{pmatrix} w_{++} & w_{+0} & w_{+-} \\ w_{0+} & w_{00} & w_{0-} \\ w_{-+} & w_{-0} & w_{--} \end{pmatrix},$$

and these inequalities follow from its positive semi-definiteness:

$$w_{00}, w_{++}, w_{--} \geq 0 \quad (11a)$$

$$\begin{vmatrix} w_{++} & w_{+0} \\ w_{0+} & w_{00} \end{vmatrix} \geq 0 \quad (11b)$$

$$\begin{vmatrix} w_{00} & w_{0-} \\ w_{-0} & w_{--} \end{vmatrix} \geq 0 \quad (11c)$$

$$\begin{vmatrix} w_{++} & w_{+-} \\ w_{-+} & w_{--} \end{vmatrix} \geq 0 \quad (11d)$$

$$\begin{vmatrix} w_{++} & w_{+0} & w_{+-} \\ w_{0+} & w_{00} & w_{0-} \\ w_{-+} & w_{-0} & w_{--} \end{vmatrix} \geq 0, \quad (11e)$$

Using hermiticity and parity conservation (Eqs. (13,15) of Ref. [2]), we reduce the number of independent real parameters in the virtual photon density matrix to five:  $w_{00}, w_{++}, w_{+-}, \text{Re}w_{0+}, \text{Im}w_{0+}$ . Then the inequalities (11b-e) become

$$\begin{vmatrix} w_{++} & w_{0+}^* \\ w_{0+} & w_{00} \end{vmatrix} \geq 0 \quad (12a)$$

$$\begin{vmatrix} w_{++} & w_{+-} \\ w_{+-}^* & w_{++} \end{vmatrix} \geq 0 \quad (12b)$$

$$\begin{vmatrix} w_{++} & w_{0+}^* & w_{+-} \\ w_{0+} & w_{00} & -w_{0+} \\ w_{+-}^* & -w_{0+}^* & w_{++} \end{vmatrix} \geq 0, \quad (12c)$$

which leads immediately to the inequalities Eq. (8a,b,c). This proves the equivalence of the Cartesian general response tensor method, and the helicity density matrix method for unpolarized structure functions.

This, the second, method is based on the observation that all that is necessary is an explicit representation of the density matrix in terms of the observables, *i.e.*, coincidence structure functions. The method by which we arrive at this relationship between the density matrix elements and structure functions is irrelevant. One way is to use a general response tensor for the reaction and work out all structure functions and density matrix elements in terms of the general response functions. This provides a relation between the density matrix elements and the observables, as desired. But, that method becomes increasingly complicated as one introduces spin [17]. Hence, in the future we shall only use the simpler helicity amplitude method, but shall compare with the results of other methods whenever possible.

### 3. Discussion

The first two inequalities (8a,b) are trivial: they are equivalent to the statement that the sums of squares of amplitudes have to be positive or zero. The next inequality stating that the transverse structure function is larger or equal to the absolute value of the transverse-transverse interference structure function is not very surprising, but it was not well-known either. The fourth result is a non-trivial inequality involving all five structure functions appearing in the unpolarized cross section, that has not been investigated or applied to models, so far. It can be used to set bounds on one of the structure functions if the other four are known. For example, in the so called impulse approximation the fifth structure function  $R_{LT'}^{(I)}$  vanishes identically. We know that this result is unrealistic because all final state interactions are neglected there. But from the knowledge of  $R_L$ ,  $R_T$ ,  $R_{TT}^{(I)}$ ,  $R_{LT}^{(I)}$  we can obtain an upper bound on the size of  $R_{LT'}^{(I)}$  in a more realistic approximation:

$$|R_{LT'}^{(I)}| \leq \sqrt{4R_L(R_T - R_{TT}^{(I)}) - (R_{LT}^{(I)})^2}.$$

These inequalities were first derived in Ref. [17], but they remained largely unknown in the nuclear physics community. They might prove to be of practical importance as consistency checks of the experimental extraction procedure for coincidence observables.

The other possibility is to use a specific reaction whose density matrix can be unambiguously expressed in terms of its structure functions. This can be done as long as all possible structure functions are represented, *i.e.*, none of them vanish “by accident”. The structure

function inequalities obtained in this way are the same as the inequalities obtained from the general response tensor.

From now on, we will use only the second, or density matrix, method for the derivation of the polarized structure function inequalities. Some of the polarized-target inequalities to be derived have been known for some time (Ref. [17]), but many more are new.

### III. POLARIZED COINCIDENCE STRUCTURE FUNCTION INEQUALITIES

If another spin degree of freedom, besides that of the photon, is available, the density matrix becomes the direct product of the two density matrices and consequently increases in size to  $3(2s+1) \times 3(2s+1)$ , where  $s$  is the (additionally) observed spin. Just as in Sec. II, the elements of this density matrix are bilinear products of the electromagnetic current induced transition amplitudes, so that they also can be expressed in terms of the inelastic electron scattering polarization observables. The condition for this density matrix to be positive semi-definite leads to a multitude of inequalities among the polarized structure functions. Once again, the resulting inequalities are independent of the specific basis vectors chosen in the Hilbert space. Certain bases, however, are more suitable for an easy evaluation of the inequalities than others. The substantial simplification that comes about due to the use of transversity amplitudes [21] was observed in Ref. [17,12,22].

The method used to find the relationship between the density matrix elements and the observables (structure functions) is unimportant. The “canonical” method [12] is to expand the response tensor in all possible Lorentz covariants consistent with the general principles, such as the current conservation, hermiticity, and parity conservation. Then one expresses the structure functions  $R$ ’s in terms of the response tensor functions. After writing the density matrix elements in terms of the response tensor matrix elements, one can express the density matrix elements in terms of the observables. Application of the positivity constraints to the density matrix then automatically leads to inequalities among the structure functions.

Instead of using this rather cumbersome approach, we choose a specific process belonging to the given category (*i.e.*, having the required spin degrees of freedom) and then evaluate its response functions in terms of a finite number of transition amplitudes. By expressing the density matrix elements in terms of these very same transition amplitudes one gets a one-to-one relationship between the density matrix elements and the observables. The only danger in this procedure is in choosing a reaction that does not allow a unique assignment of observables to the density matrix elements. An example of such a case would be to take a reaction that has too few independent amplitudes, such as the completely spinless reaction, in order to determine the unpolarized structure function inequalities. We know that, in this case, all amplitudes can be completely separated from the five unpolarized structure functions [2]. But, due to this simplicity, one structure function is linearly dependent,  $R_T = \pm R_{TT}$ , where the sign depends on the “parity factor”  $\eta_g = \pm$  of the reaction, so that one has an ambiguity as to which one of the two observables to use in the density matrix. The solution to this problem is to use a reaction which does *not allow a complete separation of amplitudes from the given set of observables*. In this way one ensures absence of ambiguities and the results one obtains are the same as those obtained by using the general response tensor method, but with a bigger effort.

In the case of the spin 1/2 target or recoil polarization measurements, an example of such a “sample” reaction is scalar or pseudoscalar electroproduction off a spin 1/2 target. It was proven in Ref. [8] that the amplitudes of this reaction cannot be completely separated from only one of these two sets of measurements; thus there is no danger of ambiguity. Secondly, all of the observables for these two cases have already been worked out in terms of the transition amplitudes in Ref. [8]. There only remains the task of expressing the density matrices in terms of amplitudes, which is accomplished in the next subsection.

### A. Polarization observables for spin 1/2 particle target and ejectile electroproduction

We will present the results for  $\vec{p}(e, e'\vec{p})\pi$  reaction in order to illustrate the method. In order to write the density matrix elements for  $\vec{p}(e, e'\vec{p})\pi$  in terms of observables, we will use the results of Ref. [8], as expressed in the notation of Ref. [2]. That allows a simple extension of this method to the  $\vec{d}(e, e'\vec{p})n$  reaction, as well. Experience has shown that certain linear combinations of helicity amplitudes, called hybrid amplitudes, greatly simplify the resulting tables of observables. These amplitudes are constructed from transversity states [21], whose spin quantization axis is perpendicular to the reaction plane, for all particles in the reaction except the virtual photon. In our case this axis is the  $y' = y''$  direction (Fig. 1). Moreover, the transition from the helicity to the transversity states is accomplished by a unitary transformation that leaves the positivity properties of the density matrix intact. The six independent helicity amplitudes are

$$\begin{aligned} F_1 &= \langle -\frac{1}{2} | J \cdot \epsilon_+ | -\frac{1}{2} \rangle & F_2 &= \langle -\frac{1}{2} | J \cdot \epsilon_+ | +\frac{1}{2} \rangle \\ F_3 &= \langle +\frac{1}{2} | J \cdot \epsilon_+ | -\frac{1}{2} \rangle & F_4 &= \langle +\frac{1}{2} | J \cdot \epsilon_+ | +\frac{1}{2} \rangle \\ F_5 &= \langle +\frac{1}{2} | J \cdot \epsilon_o | +\frac{1}{2} \rangle & F_6 &= \langle +\frac{1}{2} | J \cdot \epsilon_o | -\frac{1}{2} \rangle \quad , \end{aligned} \quad (13)$$

where  $J \cdot \epsilon_\lambda = J_\mu \epsilon_\lambda^\mu$  and the initial and final states are helicity states with helicities specified above, where the nucleon is particle No. 1 in the final state, as defined by Jacob and Wick [5].  $J^\mu$  is the hadronic response current defined in the ejectile plane, with Bjorken and Drell metric [18] and  $\epsilon_\pm^\mu = (0, \hat{\epsilon}_\pm)$ ,  $\epsilon_0^\mu = (1, \mathbf{0}) = (1, 0, 0, 0)$  in the c.m. frame.

The results are shown in Tables V and VI. Each structure function appears in the cross section Eq. (1) multiplied by its spin polarization vector (cf. Eq.(79) of [2]) , *e.g.*,

$$R_{LT}^{(I)} = 2\kappa^2 \sum_{i,j} p_i P_j R_{LT}^{(I)}(p_i, P_j) \quad ,$$

where

$$R_{LT}(U, U) = R_{LT} \quad (14a)$$

$$R_{LT}(U, P_n) = R_{LT}(n) \quad (14b)$$

$$R_{LT}(p_x, U) = R_{LT}(x) \quad , \quad (14c)$$

and

$$a_1 = \frac{1}{2} (|g_5|^2 + |g_6|^2) \quad , \quad a_2 = \frac{1}{2} (|g_5|^2 - |g_6|^2) \quad (15a)$$

$$b_1 = |g_1|^2 + |g_2|^2 + |g_3|^2 + |g_4|^2 \quad (15b)$$

$$b_2 = -|g_1|^2 - |g_2|^2 + |g_3|^2 + |g_4|^2 \quad (15c)$$

$$b_3 = |g_1|^2 - |g_2|^2 + |g_3|^2 - |g_4|^2 \quad (15d)$$

$$b_4 = -|g_1|^2 + |g_2|^2 + |g_3|^2 - |g_4|^2 \quad (15e)$$

$$c_1 = g_4^* g_1 + g_3^* g_2, \quad c_2 = g_4^* g_1 - g_3^* g_2 \quad (15f)$$

$$d_1 = g_4^* g_5 + g_3^* g_6, \quad d_2 = g_4^* g_5 - g_3^* g_6 \quad (15g)$$

$$e_1 = g_1^* g_5 + g_2^* g_6, \quad e_2 = g_1^* g_5 - g_2^* g_6 \quad (15h)$$

$$f_1 = g_3^* g_5 + g_4^* g_6, \quad f_2 = g_3^* g_5 - g_4^* g_6 \quad (15i)$$

$$k_1 = g_1^* g_3 + g_2^* g_4, \quad k_2 = g_1^* g_3 - g_2^* g_4, \quad (15j)$$

We are not interested in complete separation of amplitudes as in Ref. [8,2], but rather in separation of certain bilinear products that appear in density matrices to be defined below (see Eqs. (17a,b)). One can see from Tables V and VI that the moduli squared of the amplitudes are readily separable from  $a_i$ ,  $b_j$ , ( $i = 1, 2$ ) ( $j = 1, \dots, 4$ ), and the same holds for the aforementioned bilinear products. An analogous analysis of the  $d(e, e'N)N'$  reaction was presented in Ref. [2]. That provides the necessary information for the construction of  $s = 1$  polarized target inequalities.

## B. Derivation of polarized positivity inequalities

In the case of reactions with spin, the electromagnetic current matrix elements  $J_a$  can be assembled into (not necessarily square) matrices. The density matrix with final state spin indices (ejectile polarization)

$$\rho_{\lambda\lambda', tt'}^f = \begin{pmatrix} J_+ J_+^\dagger & J_+ J_0^\dagger & J_+ J_-^\dagger \\ J_0 J_+^\dagger & J_0 J_0^\dagger & J_0 J_-^\dagger \\ J_- J_+^\dagger & J_- J_0^\dagger & J_- J_-^\dagger \end{pmatrix}$$

is positive semidefinite [23], just like the initial state density matrix (target polarization)

$$\rho_{\lambda\lambda', t't}^i = \begin{pmatrix} J_+^\dagger J_+ & J_+^\dagger J_0 & J_+^\dagger J_- \\ J_0^\dagger J_+ & J_0^\dagger J_0 & J_0^\dagger J_- \\ J_-^\dagger J_+ & J_-^\dagger J_0 & J_-^\dagger J_- \end{pmatrix}.$$

We are free to apply similarity transformations to this density matrix because it will not change its positivity properties. This allows us to change the transverse photon helicity matrix elements to a new set described below. We are also free to choose any spin quantization axis; a particularly convenient one will turn out to be the normal to the ejectile plane. This leads to transversity states [21]. We will refer to amplitudes  $g_i$  as the hybrid amplitudes, because the photon state is described by its helicity, while all other states are transversity states. The longitudinal hybrid amplitudes for pseudoscalar electroproduction off an  $s = 1/2$  target are defined as follows (for details of this construction see Ref. [2,8]):

$$J_o = \begin{pmatrix} g_5 & 0 \\ 0 & g_6 \end{pmatrix}. \quad (16a)$$

The transverse hybrid amplitudes can be represented by the following two matrices:

$$J_s = \frac{1}{2}(J_+ - J_-) = \begin{pmatrix} 0 & g_4 \\ g_3 & 0 \end{pmatrix} \quad (16b)$$

$$J_a = \frac{1}{2}(J_+ + J_-) = \begin{pmatrix} g_1 & 0 \\ 0 & g_2 \end{pmatrix}. \quad (16c)$$

The specific linear combinations which define the  $g$ 's are given in Sec. III.A, as are the definitions of helicity amplitudes and the tables of observables. It is now straightforward to construct the transformed final state (recoil polarization) density matrix:

$$\rho_{ab,tt'}^f = \begin{pmatrix} J_a J_a^\dagger & J_a J_o^\dagger & J_a J_s^\dagger \\ J_o J_a^\dagger & J_o J_o^\dagger & J_o J_s^\dagger \\ J_s J_a^\dagger & J_s J_o^\dagger & J_s J_s^\dagger \end{pmatrix} \quad (17a)$$

and the initial state (target polarization) density matrix:

$$\rho_{ba,tt'}^i = \begin{pmatrix} J_a^\dagger J_a & J_a^\dagger J_o & J_a^\dagger J_s \\ J_o^\dagger J_a & J_o^\dagger J_o & J_o^\dagger J_s \\ J_s^\dagger J_a & J_s^\dagger J_o & J_s^\dagger J_s \end{pmatrix}. \quad (17b)$$

The block matrices are

$$J_o J_o^\dagger = \begin{pmatrix} |g_5|^2 & 0 \\ 0 & |g_6|^2 \end{pmatrix} = J_o^\dagger J_o \quad (18a)$$

$$J_s J_s^\dagger = \begin{pmatrix} |g_1|^2 & 0 \\ 0 & |g_2|^2 \end{pmatrix} = J_s^\dagger J_s \quad (18b)$$

$$J_a J_a^\dagger = \begin{pmatrix} |g_4|^2 & 0 \\ 0 & |g_3|^2 \end{pmatrix} \quad (18c)$$

$$J_a^\dagger J_a = \begin{pmatrix} |g_3|^2 & 0 \\ 0 & |g_4|^2 \end{pmatrix} \quad (18d)$$

$$J_o J_s^\dagger = \begin{pmatrix} g_5 g_1^* & 0 \\ 0 & g_6 g_2^* \end{pmatrix} \quad (18e)$$

$$J_s J_a^\dagger = \begin{pmatrix} 0 & g_1 g_3^* \\ g_2 g_4^* & 0 \end{pmatrix} \quad (18f)$$

$$J_o J_a^\dagger = \begin{pmatrix} 0 & g_5 g_3^* \\ g_6 g_4^* & 0 \end{pmatrix} \quad (18g)$$

and similarly for other  $2 \times 2$  block matrices that appear in the density matrices  $\rho_{f,i}$  Eq. (17a,b). We will express these matrix elements in terms of observables by using Tables V and VI in Sec. III.A, or Ref. [8]. As an example of derivation, we look at the principal minors of the diagonal submatrix  $J_o J_o^\dagger$  Eq. (17a); we use Table VI and Eq. (15a,b) to find the two inequalities

$$\begin{aligned} R_L(U) &\geq -R_L(n) \\ R_L(U) &\geq R_L(n), \end{aligned}$$

which immediately lead to

$$R_L(U) \geq |R_L(n)|.$$

Similarly straightforward applications of the positivity conditions to other  $2 \times 2$  and  $4 \times 4$  diagonal submatrices of the initial and final state density matrices lead immediately to Eqs. (19,20). Clearly, the larger the submatrix, the more powers of structure functions in the inequalities, the highest power in this case being six.

### C. Polarized spin 1/2 target and ejectile positivity inequalities

We start with target polarization inequalities, some of which have been derived before in Ref. [12], which results give us another check of the method.

#### 1. Polarized target inequalities

Proceeding as in Sec. III.B, we find:

$$R_L(U) \geq |R_L(y)| \quad (19a)$$

$$R_T(U) \geq |R_T(y)| \quad (19b)$$

$$R_T(U) \geq |R_{TT}^{(I)}(y)| \quad (19c)$$

$$R_T(U) - R_{TT}^{(I)}(U) \geq |R_T(y) - R_{TT}^{(I)}(y)| \quad (19d)$$

$$R_T(U) + R_{TT}^{(I)}(U) \geq |R_T(y) + R_{TT}^{(I)}(y)|. \quad (19e)$$

These are the lowest order inequalities that were derived from the “smallest” minors of three diagonal block submatrices. From the next “larger” minors we find the following second order inequalities:

$$\begin{aligned} & \left[ R_T(U) + R_T(y) \right]^2 - \left[ R_{TT}^{(I)}(U) + R_{TT}^{(I)}(y) \right]^2 \geq \\ & \geq \left[ R_{T'}(x) - R_{TT}^{(II)}(z) \right]^2 + \left[ R_{TT}^{(II)}(x) + R_{T'}(z) \right]^2 \end{aligned} \quad (19f)$$

$$\begin{aligned} & \left[ R_T(U) - R_T(y) \right]^2 - \left[ R_{TT}^{(I)}(U) - R_{TT}^{(I)}(y) \right]^2 \geq \\ & \geq \left[ R_{T'}(x) + R_{TT}^{(II)}(z) \right]^2 + \left[ R_{TT}^{(II)}(x) - R_{T'}(z) \right]^2 \end{aligned} \quad (19g)$$

$$\begin{aligned} & 4 \left[ R_T(U) - R_{TT}^{(I)}(U) - R_T(y) + R_{TT}^{(I)}(y) \right] \left( R_L(U) - R_L(y) \right) \geq \\ & \geq \left[ R_{LT}^{(I)}(U) - R_{LT}^{(I)}(y) \right]^2 + \left[ R_{LT'}^{(I)}(U) - R_{LT'}^{(I)}(y) \right]^2 \end{aligned} \quad (19h)$$

$$\begin{aligned} & 4 \left[ R_T(U) - R_{TT}^{(I)}(U) + R_T(y) - R_{TT}^{(I)}(y) \right] \left( R_L(U) + R_L(y) \right) \geq \\ & \geq \left[ R_{LT}^{(I)}(U) + R_{LT}^{(I)}(y) \right]^2 + \left[ R_{LT'}^{(I)}(U) + R_{LT'}^{(I)}(y) \right]^2 \end{aligned} \quad (19i)$$

$$\begin{aligned} & 4 \left[ R_T(U) + R_{TT}^{(I)}(U) + R_T(y) + R_{TT}^{(I)}(y) \right] \left( R_L(U) - R_L(y) \right) \geq \\ & \geq \left[ R_{LT}^{(II)}(x) - R_{LT}^{(II)}(z) \right]^2 + \left[ R_{LT'}^{(II)}(x) + R_{LT'}^{(II)}(z) \right]^2 \end{aligned} \quad (19j)$$

$$\begin{aligned} & 4 \left[ R_{T'}(U) + R_{TT}^{(I)}(U) - R_T(y) - R_{TT}^{(I)}(y) \right] \left( R_L(U) + R_L(y) \right) \geq \\ & \geq \left[ R_{LT}^{(II)}(x) + R_{LT}^{(II)}(z) \right]^2 + \left[ R_{LT'}^{(II)}(x) - R_{LT'}^{(II)}(z) \right]^2 \end{aligned} \quad (19k)$$

where  $x$ ,  $y$ ,  $z$  stand for target polarization vector components along the  $x'$ ,  $y'$ ,  $z'$  directions (Fig. 1), respectively.

Comparison with the results of Ref. [12] is not straightforward for the following reasons: (i) some of their inequalities were derived with additional special assumptions such as that the longitudinal structure function vanish  $W_s = \left(1 - \frac{\nu^2}{q^2}\right) W_2 - W_1 = 0$  (Sec. IV of [12]), (ii) the coordinate frame with respect to which the target polarization is defined is different ( $x \leftrightarrow \pm y$ ) from ours. We only look at those inequalities that can be readily compared. We find that Eqs. (A 20 a,b,c) of [12] correspond exactly to our Eqs. (19 e,h,i), respectively. The two “trivial Schwarz” inequalities (3.7) of Ref. [12] can be derived from our Eqs. (19 f,g) and Eqs. (19 h-k), but not *vice versa*, for which reason we do not consider them as independent results. Furthermore, De Rujula, Doncel and de Rafael quote three third-order inequalities (their Eqs.(3.6, A 18, A 19)) which are beyond the scope of this paper. That leaves us with eight new first- and second-order polarized target inequalities.

## 2. Polarized ejectile inequalities

Relating the density matrix elements and the observables and proceeding as in Sec. III.B, we obtain the following inequalities for recoil polarization structure functions:

$$R_L(U) \geq |R_L(n)| \quad (20a)$$

$$R_T(U) \geq |R_T(n)| \quad (20b)$$

$$R_T(U) \geq |R_{TT}^{(I)}(n)| \quad (20c)$$

$$R_T(U) - R_{TT}^{(I)}(U) \geq |R_T(n) - R_{TT}^{(I)}(n)| \quad (20d)$$

$$R_T(U) + R_{TT}^{(I)}(U) \geq |R_T(n) + R_{TT}^{(I)}(n)| \quad (20e)$$

$$\begin{aligned} & \left[ R_T(U) - R_T(n) \right]^2 - \left[ R_{TT}^{(I)}(U) - R_{TT}^{(I)}(n) \right]^2 \geq \\ & \geq \left[ R_{T'}(s) + R_{TT}^{(II)}(l) \right]^2 + \left[ R_{TT}^{(II)}(s) - R_{T'}(l) \right]^2 \end{aligned} \quad (20f)$$

$$\begin{aligned} & \left[ R_T(U) + R_T(n) \right]^2 - \left[ R_{TT}^{(I)}(U) + R_{TT}^{(I)}(n) \right]^2 \geq \\ & \geq \left[ R_{T'}(s) - R_{TT}^{(II)}(l) \right]^2 + \left[ R_{TT}^{(II)}(s) + R_{T'}(l) \right]^2 \end{aligned} \quad (20g)$$

$$\begin{aligned} & 4 \left[ R_T(U) - R_{TT}^{(I)}(U) - R_T(n) + R_{TT}^{(I)}(n) \right] \left( R_L(U) - R_L(n) \right) \geq \\ & \geq \left[ R_{LT}^{(I)}(U) - R_{LT}^{(I)}(n) \right]^2 + \left[ R_{LT'}^{(I)}(U) - R_{LT'}^{(I)}(n) \right]^2 \end{aligned} \quad (20h)$$

$$\begin{aligned} & 4 \left[ R_T(U) - R_{TT}^{(I)}(U) + R_T(n) - R_{TT}^{(I)}(n) \right] \left( R_L(U) + R_L(n) \right) \geq \\ & \geq \left[ R_{LT}^{(I)}(U) + R_{LT}^{(I)}(n) \right]^2 + \left[ R_{LT'}^{(I)}(U) + R_{LT'}^{(I)}(n) \right]^2 \end{aligned} \quad (20i)$$

$$\begin{aligned} & 4 \left[ R_T(U) + R_{TT}^{(I)}(U) + R_T(n) + R_{TT}^{(I)}(n) \right] \left( R_L(U) + R_L(n) \right) \geq \\ & \geq \left[ R_{LT'}^{(II)}(s) + R_{LT}^{(II)}(l) \right]^2 + \left[ R_{LT}^{(II)}(s) - R_{LT'}^{(II)}(l) \right]^2 \end{aligned} \quad (20j)$$



$$\begin{aligned}
& 4 \left[ R_T(U) + R_{TT}^{(I)}(U) - R_T(n) - R_{TT}^{(I)}(n) \right] \left( R_L(U) - R_L(n) \right) \geq \\
& \geq \left[ R_{LT'}^{(II)}(s) - R_{LT'}^{(II)}(l) \right]^2 + \left[ R_{LT}^{(II)}(s) + R_{LT}^{(II)}(l) \right]^2,
\end{aligned} \tag{20k}$$

where  $s$ ,  $n$ ,  $l$  stand for recoil polarization vector components along the  $x''$ ,  $y''$ ,  $z''$  directions (Fig. 1), respectively. All of the polarized ejectile results are new, to the best of our knowledge, and they hold in all  $s = 1/2$  ejectile reactions, such as  $d(e, e'\vec{p})n$ , and not just in  $p(e, e'\vec{p})\pi$ , from which they were derived.

### 3. Discussion

Note that these are the inequalities that were obtained from minors of the two lowest-order diagonal block submatrices. The density matrix is  $6 \times 6$  dimensional now, so there are inequalities with products of up to six response functions ( $6^{th}$  order). Some of these inequalities, however, may turn out to be just products of lower order inequalities and hence trivial.

The higher order inequalities will be useless for some time to come, because they involve large numbers of spin observables that are not likely to be measured soon. The high degree of nonlinearity makes them quite unlikely to be useful for setting up bounds on other observables. For these reasons they are omitted from this work.

Finally, we see that this method can be readily applied to  $s = 1$  polarized target structure functions as well. The procedure is the same as outlined in Sec. III.B above: construct the initial state density matrix  $\rho_i$  Eq. (17b) out of hybrid amplitude matrices  $J_o, J_a, J_s$ , shown in Eqs (67,69,70) of Ref. [2], and then set its principal minors larger or equal to zero. Write the matrix elements of  $\rho_i$  in terms of polarized target structure functions given in Tables X, XI and XII, to find the desired results. Since polarized deuteron target measurements are not bound to be made soon, we do not derive such inequalities here.

To summarize, in this paper we have derived three known and 19 new inequalities among the polarized coincidence inelastic electron scattering structure functions, assuming that the polarized target, or the polarized ejectile, has spin  $1/2$ . A large number of such inequalities have been left for the reader to derive with the help of rules developed here. This paper completes the development of helicity formalism as applied to polarized coincidence electron scattering.

### ACKNOWLEDGMENTS

The author would like to acknowledge useful conversations with O. Hanstein and would like to thank Prof. R. Brockmann for his hospitality at the University of Mainz on two occasions in the summer and fall of 1992, which greatly facilitated the inception of this paper. This work was partially supported by SURA through a CEBAF fellowship.

## APPENDIX A: RELATION BETWEEN HELICITY AND TRANSVERSITY AMPLITUDES

The connection between the hybrid amplitudes  $g_i$  and the helicity amplitudes  $F_i$  can be summarized by the matrix relation

$$g_i = \Lambda_{ij} F_j ,$$

where, for transverse amplitudes ( $i, j = 1-4$ ), while for longitudinal amplitudes ( $i, j=5-6$ ) and

$$\Lambda_{ij} = \frac{1}{2} \begin{pmatrix} 1 & i & -i & 1 & 0 & 0 \\ 1 & -i & i & 1 & 0 & 0 \\ -i & 1 & 1 & i & 0 & 0 \\ i & 1 & 1 & -i & 0 & 0 \\ 0 & 0 & 0 & 0 & 2 & -2i \\ 0 & 0 & 0 & 0 & 2 & 2i \end{pmatrix} .$$

## REFERENCES

- [1] W.E. Kleppinger and J.D. Walecka, Ann. Phys. **146**, 349 (1983); ibid. **151**, 497(E) (1983).
- [2] V. Dmitrašinović and Franz Gross, Phys. Rev. C **40**, 2479 (1989); Phys. Rev. C **43**, 1495(E) (1991).
- [3] A.S. Raskin and T.W. Donnelly, Ann. Phys. **191**, 78 (1989).
- [4] A. Pickelsimer and J.W. van Orden, Phys. Rev. C **40**, 290 (1989).
- [5] M. Jacob and G.C. Wick, Ann. Phys. **7**, 404 (1959); see also C. Kuang-Chao and M.I. Shirokov, Sov. Phys. JETP **7**, 851 (1958) and references cited therein.
- [6] F.M. Renard, J. Tran Thanh Van and M. Le Bellac, Nuovo Cimento **38**, 552 (1965); **38**, 1688 (1965).
- [7] J.D. Walecka and P.A. Zucker, Phys. Rev. **167**, 1479 (1968).
- [8] V. Dmitrašinović, T.W. Donnelly and Franz Gross, “Research Program at CEBAF (III), RPAC III”, published by CEBAF (Jan. 1988), ed. F. Gross, p. 547; ibid, Report of the CEBAF Out-of-Plane Task Force, p. 183.
- [9] V. Dmitrašinović, College of William and Mary Ph.D. Thesis (1990).
- [10] V. Dmitrašinović, Phys. Rev. C **47**, 2195 (1993).
- [11] T. de Forest and J.D. Walecka, Adv. in Phys. **15**, 1 (1966).
- [12] A. De Rujula, M.G. Doncel and E. de Rafael, Phys. Rev. D **8**, 839 (1973).
- [13] T. de Forest, Ann. Phys. **45**, 365 (1967).
- [14] H. Arenhövel, W. Leidemann, E.L. Tomusiak, Phys. Rev. C **46**, 455 (1992).
- [15] B. Mosconi, J. Pauschenwein and P. Ricci, Phys. Rev. C **48**, 332 (1993).
- [16] M.G. Doncel and E. de Rafael, Nuov. Cim. **4A**, 363 (1971).
- [17] A. De Rujula and E. de Rafael, Ann. Phys. **78**, 132 (1973).
- [18] J.D. Bjorken and S.D. Drell *Relativistic Quantum Mechanics* (McGraw-Hill, 1964).
- [19] R. W. Lourie, Nucl. Phys. **A 509**, 653 (1990); Z. Phys. C **50**, 345 (1991).
- [20] O. Hanstein, see section 5 of *Polarisationsfreiheitsgrade bei der Elektroproduktion von Pionen am Nukleon*, Johannes Gutenberg-Universität Mainz, Diplomarbeit (1993) (in German); also private communication.
- [21] A. Kotanski, Acta Phys. Pol. **29**, 699 (1966); **30**, 629 (1966).
- [22] I.S. Barker, A. Donnachie and J.K. Storrow, Nucl. Phys. **B95** (1975) 347.
- [23] C. Bourrely, E. Leader and J. Soffer, Phys. Rep. **59**, 95 (1980).

# FIGURES

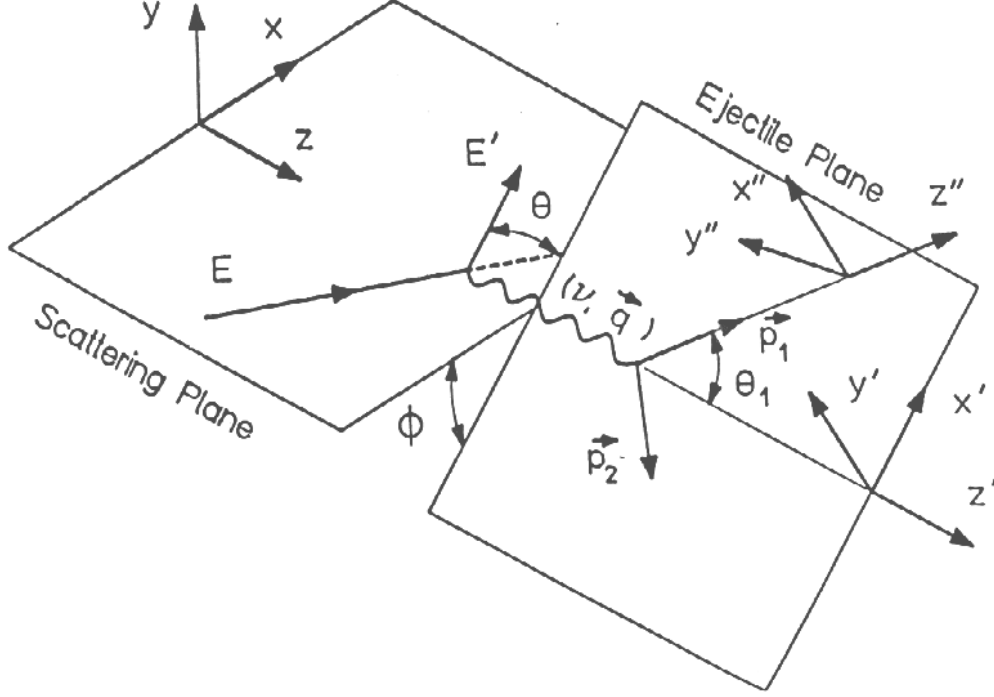


FIG. 1. Geometry of the coincidence electroproduction or electrodisintegration process showing the electron scattering plane, the ejectile plane, and the two coordinate systems in the ejectile plane:  $(x', y', z')$  defined by the virtual photon's three momentum  $\mathbf{q}_L$  which is parallel to the  $z, z'$  axes, and  $(x'', y'', z'')$  where  $z''$  is along the ejectile three-momentum  $\mathbf{p}_1$ . The axes  $y', y''$  are perpendicular to the ejectile plane. The axis  $y$  is perpendicular to the electron scattering plane.

# TABLES

TABLE I. Structure functions  $R_{ij}$  expressed in terms of the response tensor components (second column) or helicity amplitudes (third column), where  $\kappa^2 = \frac{1}{4\pi^2} \left( \frac{M_1 M_2}{2W} \right)$  for both electroproduction and deuteron electrodisintegration [2]. The helicity amplitudes are defined in the c.m. frame as follows:  $J_{\pm} = J \cdot \epsilon_{\pm} = -\vec{J} \cdot \hat{\epsilon}_{\pm}$  and  $J^o$  is the zeroth component of the four-vector  $J^{\mu}$  in the c.m. frame. The subscript 0 in  $R_{ij}$ 's in the second column corresponds to covariant helicity zero states and  $1/\eta = (\frac{W}{M_T})(\frac{Q}{q_L})$  in the c.m. frame [2].

$R_L$	$\eta^2 R_{oo}$	$\kappa^2 \sum  J^o ^2$
$R_T$	$R_{++} + R_{--}$	$\kappa^2 \sum ( J_+ ^2 +  J_- ^2)$
$R_{TT}^{(I)}$	$2\text{Re}R_{+-}$	$2\kappa^2 \text{Re} \sum (J_+ J_-^{\dagger})$
$R_{TT}^{(II)}$	$-2\text{Im}R_{+-}$	$-2\kappa^2 \text{Im} \sum (J_+ J_-^{\dagger})$
$R_{LT}^{(I)}$	$2\eta \text{Re}(R_{o+} - R_{o-})$	$2\kappa^2 \text{Re} \sum J^o (J_+^{\dagger} - J_-^{\dagger})$
$R_{LT}^{(II)}$	$2\eta \text{Im}(R_{o+} + R_{o-})$	$2\kappa^2 \text{Im} \sum J^o (J_+^{\dagger} + J_-^{\dagger})$
$R_{T'}$	$R_{++} - R_{--}$	$\kappa^2 \sum ( J_+ ^2 -  J_- ^2)$
$R_{LT'}^{(II)}$	$2\eta \text{Re}(R_{o+} + R_{o-})$	$2\kappa^2 \text{Re} \sum J^o (J_+^{\dagger} + J_-^{\dagger})$
$R_{LT'}^{(I)}$	$2\eta \text{Im}(R_{o+} - R_{o-})$	$2\kappa^2 \text{Im} \sum J^o (J_+^{\dagger} - J_-^{\dagger})$

TABLE II. Unpolarized inelastic coincidence structure functions  $R$ 's in the lab frame expressed in terms of the general response tensor functions  $W_i, i = 1 - 5$ . Here  $c = 1 - \left( \frac{\nu p_1}{q_L E_1} \right) \cos \theta_1^L$ .

$R_L$	$\left( \frac{q_L}{Q} \right)^2 \left\{ -W_1 + \left( \frac{q_L}{Q} \right)^2 [W_2 + cW_3 + c^2W_4] \right\}$
$R_T$	$2W_1 + W_4 \left( \frac{p_1}{M} \sin \theta_1 \right)^2$
$R_{TT}^{(I)}$	$-W_4 \left( \frac{p_1}{M} \sin \theta_1 \right)^2$
$R_{LT}^{(I)}$	$\sqrt{2} \left( \frac{q_L}{Q} \right)^2 \left( \frac{p_1}{E_1} \sin \theta_1 \right) [W_3 + 2c \left( \frac{E_1}{M} \right)^2 W_4]$
$R_{LT'}^{(I)}$	$\sqrt{2} \left( \frac{q_L}{Q} \right)^2 \left( \frac{p_1}{E_1} \sin \theta_1 \right) W_5$

TABLE III. Structure functions  $R$ 's (first column) as functions of the response tensor components in the helicity basis (second column), or as functions of the general response tensor Cartesian components (third column) defined in the Breit frame and in the ejectile plane of Fig. 1; all other elements of the general response tensor, e.g.  $w_{xy}$ ,  $w_{0y}$  are zero. In the Breit frame  $\eta = 1$ .

$R_L$	$\eta^2 R_{oo}$	$\eta^2 w_{00}^B$
$R_T$	$R_{++} + R_{--}$	$w_{xx} + w_{yy}$
$R_{TT}^{(I)}$	$2\text{Re}R_{+-}$	$w_{yy} - w_{xx}$
$R_{TT}^{(II)}$	$-2\text{Im}R_{+-}$	0
$R_{LT}^{(I)}$	$2\eta\text{Re}(R_{o+} - R_{o-})$	$2\sqrt{2}\eta\text{Re}w_{ox}^B$
$R_{LT}^{(II)}$	$2\eta\text{Im}(R_{o+} + R_{o-})$	0
$R_{T'}$	$R_{++} - R_{--}$	0
$R_{LT'}^{(II)}$	$2\eta\text{Re}(R_{o+} + R_{o-})$	0
$R_{LT'}^{(I)}$	$2\eta\text{Im}(R_{o+} - R_{o-})$	$2\sqrt{2}\eta\text{Im}w_{ox}^B$

TABLE IV. Structure functions  $R$ 's (first column) as functions of the response tensor components in the helicity basis (second column) or as functions of the general response tensor components in the helicity basis in the Breit frame and defined in the ejectile plane (third column). In the Breit frame  $\eta = 1$ .

$R_L$	$\eta^2 R_{oo}$	$\eta^2 w_{00}^B$
$R_T$	$R_{++} + R_{--}$	$2w_{++}$
$R_{TT}^{(I)}$	$2\text{Re}R_{+-}$	$2w_{+-}$
$R_{TT}^{(II)}$	$-2\text{Im}R_{+-}$	0
$R_{LT}^{(I)}$	$2\eta\text{Re}(R_{o+} - R_{o-})$	$4\eta\text{Re}w_{o+}^B$
$R_{LT}^{(II)}$	$2\eta\text{Im}(R_{o+} + R_{o-})$	0
$R_{T'}$	$R_{++} - R_{--}$	0
$R_{LT'}^{(II)}$	$2\eta\text{Re}(R_{o+} + R_{o-})$	0
$R_{LT'}^{(I)}$	$2\eta\text{Im}(R_{o+} - R_{o-})$	$4\eta\text{Im}w_{o+}^B$

TABLE V. Recoil polarization observables as functions of hybrid amplitudes  $g_i$ , where  $U$  stands for unpolarized and  $(P_n, P_s, P_l)$  are the  $(y, x, z)$  components, respectively, of the recoil polarization vector as measured in c.m. frame with respect to the  $(x'', y'', z'')$  coordinate frame (Fig. 1).

	U	$P_n$	$P_s$	$P_l$
$R_L$	$a_1$	$a_2$		
$R_T$	$b_1$	$b_3$		
$R_{TT}^{(I)}$	$b_2$	$b_4$		
$R_{LT}^{(I)}$	$\text{Re}(e_1)$	$\text{Re}(e_2)$		
$R_{LT'}^{(I)}$	$\text{Im}(e_1)$	$\text{Im}(e_2)$		
$R_{LT}^{(II)}$			$\text{Im}(d_1)$	$\text{Re}(d_2)$
$R_{LT'}^{(II)}$			$\text{Re}(d_1)$	$-\text{Im}(d_2)$
$R_{TT}^{(II)}$			$-\text{Im}(c_1)$	$\text{Re}(c_2)$
$R_{T'}$			$\text{Re}(c_1)$	$\text{Im}(c_2)$

TABLE VI. Same as Table V, but for polarized target observables as functions of hybrid amplitudes  $g_i$ , where  $U$  stands for unpolarized and  $(p_x, p_y, p_z)$  are the  $(x, y, z)$  components, respectively, of the target polarization vector as measured in c.m. frame with respect to the  $(x', y', z')$  coordinate frame (Fig. 1).

	U	$p_y$	$p_x$	$p_y$
$R_L$	$a_1$	$-a_2$		
$R_T$	$b_1$	$b_4$		
$R_{TT}^{(I)}$	$b_2$	$b_3$		
$R_{LT}^{(I)}$	$\text{Re}(e_1)$	$-\text{Re}(e_2)$		
$R_{LT'}^{(I)}$	$\text{Im}(e_1)$	$-\text{Im}(e_2)$		
$R_{LT}^{(II)}$			$\text{Im}(f_1)$	$\text{Re}(f_2)$
$R_{LT'}^{(II)}$			$\text{Re}(f_1)$	$-\text{Im}(f_2)$
$R_{TT}^{(II)}$			$\text{Im}(k_1)$	$-\text{Re}(k_2)$
$R_{T'}$			$\text{Re}(k_1)$	$\text{Im}(k_2)$